

SUPPORTING INFORMATION

**Precursor- and Time-Dependent Morphological Evolution of ZnO Nanostructures
for Comparative Photocatalytic Activity and Adsorption Dynamics with
Methylene Blue Dye**

Smriti Thakur and Sanjay K. Mandal*

Department of Chemical Sciences, Indian Institute of Science Education and Research Mohali,
Sector 81, Manauli PO, S.A.S. Nagar, Mohali, Punjab 140306, INDIA.

Corresponding Author

*Email: sanjaymandal@iisermohali.ac.in

Table of Contents

Item		Page No.
Table S1	Lattice parameters of as-synthesized ZnO nanostructures	S3-S5
Table S2	Band gap values of as-synthesized ZnO nanostructures	S5
Table S3	Calculated particle sizes of as-synthesized ZnO nanostructures using Meulenkamp's equation	S6
Table S4	Percent decolorization and rate constant values of as-synthesized ZnO nanostructures calcined for 12 hours	S7
Table S5	Comparison of percentage degradation efficiency of MB dye by the ZnO nanostructures with literature values	S7
Figure S1	Raman spectra of ZnO nanostructures	S8
Figure S2	Tauc plots of as-synthesized ZnO nanostructures	S8
Figure S3	Energy level diagram of as-synthesized ZnO nanostructures	S9
Figure S4-S12	Linear fit of kinetic models	S10-S18

Table S1. Lattice parameters, atomic packing fraction (APF) and interplanar spacing (d) for the as-synthesized ZnO nanostructures.^{a-c}

Sample	hkl	2θ values (degrees)	Lattice constants a, b, c (Å)	Volume of unit cell (Å ³)	APF	d values (Å)
ZnO-bpma-6	(100)	31.50	a = b = 3.28, c = 5.26	49.15	0.755	2.84
	(002)	34.15				2.63
	(101)	35.98				2.50
ZnO-bpma-12	(100)	31.52	a = b = 3.28, c = 5.25	49.05	0.755	2.84
	(002)	34.17				2.62
	(101)	36.01				2.49
ZnO-bpma-18	(100)	31.49	a = b = 3.28, c = 5.26	49.23	0.755	2.84
	(002)	34.14				2.63
	(101)	35.97				2.50
ZnO-bpma-24	(100)	31.49	a = b = 3.28, c = 5.25	49.18	0.755	2.84
	(002)	34.15				2.62
	(101)	35.98				2.50
ZnO-bpea-6	(100)	31.43	a = b = 3.29, c = 5.27	49.45	0.755	2.85
	(002)	34.09				2.63
	(101)	35.91				2.50
ZnO-bpea-12	(100)	31.50	a = b = 3.29, c = 5.26	49.34	0.755	2.85
	(002)	34.16				2.63
	(101)	35.98				2.50

ZnO-bpea-18	(100)	31.45	a = b = 3.29, c = 5.26	49.76	0.755	2.85
	(002)	34.13				2.63
	(101)	35.96				2.50
ZnO-bpea-24	(100)	31.44	a = b = 3.29, c = 5.26	49.44	0.755	2.85
	(002)	34.11				2.63
	(101)	35.92				2.50
ZnO-bpta-6	(100)	31.49	a = b = 3.29, c = 5.26	49.20	0.755	2.84
	(002)	34.12				2.63
	(101)	35.94				2.51
ZnO-bpta-12	(100)	31.46	a = b = 3.29, c = 5.26	49.33	0.755	2.84
	(002)	34.12				2.63
	(101)	35.94				2.50
ZnO-bpta-18	(100)	31.50	a = b = 3.28, c = 5.26	49.16	0.755	2.84
	(002)	34.16				2.63
	(101)	35.98				2.50
ZnO-bpta-24	(100)	31.45	a = b = 3.29, c = 5.26	49.36	0.755	2.85
	(002)	34.10				2.63
	(101)	35.94				2.50

^aThe lattice parameters for hexagonal ZnO nanoparticles were estimated from the equations below:⁵²

$$\frac{1}{d^2} = \frac{4(h^2 + hk + k^2)}{3a^2} + \frac{l^2}{c^2} \quad (\text{S1})$$

where a and c are the lattice parameters and h , k and l are the Miller indices and d_{hkl} is the interplanar spacing for the plane $(h k l)$. This interplanar spacing for the plane $(h k l)$ can be calculated from Bragg's law:

$$2d \sin \theta = n\lambda \quad (\text{S2})$$

^bThe volume (V) of the unit cell for hexagonal system can be calculated from the following equation:

$$V = 0.866 \times a^2 \times c \quad (\text{S3})$$

^cThe atomic packing fraction (APF) can be calculated using the following equation:

$$\text{APF} = \frac{2\pi a}{3\sqrt{3}c} \quad (\text{S4})$$

Table S2. Band gap values of as-synthesized ZnO nanostructures.

Sample	Band Gap (E_g) (eV)
ZnO-bpma-6	3.18
ZnO-bpma-12	3.19
ZnO-bpma-18	3.19
ZnO-bpma-24	3.20
ZnO-bpea-6	3.19
ZnO-bpea-12	3.18
ZnO-bpea-18	3.20
ZnO-bpea-24	3.19
ZnO-bpta-6	3.15
ZnO-bpta-12	3.03
ZnO-bpta-18	3.15
ZnO-bpta-24	3.17

Table S3. Calculated particle sizes of as-synthesized ZnO nanostructures from Meulenkamp's equation.

Sample	Particle Size (nm)
ZnO-bpma-6	67
ZnO-bpma-12	67
ZnO-bpma-18	73
ZnO-bpma-24	171
ZnO-bpea-6	56
ZnO-bpea-12	55
ZnO-bpea-18	56
ZnO-bpea-24	62
ZnO-bpta-6	60
ZnO-bpta-12	68
ZnO-bpta-18	70
ZnO-bpta-24	74

Table S4. Percentage decolorization and the rate constants of ZnO-bpma-12, ZnO-bpea-12 and ZnO-bpta-12 at different time intervals.

Time (min)	% decolorization ZnO-bpma-12	Rate Constant (min ⁻¹)	% decolorization ZnO-bpea-12	Rate Constant (min ⁻¹)	% decolorization ZnO-bpta-12	Rate Constant (min ⁻¹)
0	0	0	0	0	0	0
60	40	0.00852	13	0.00236	55	0.01353
120	49	0.00562	22	0.00211	67	0.00933
180	63	0.00554	27	0.00173	76	0.00800
240	71	0.00514	34	0.00172	81	0.00688
300	79	0.00529	38	0.00160	84	0.00613
360	86	0.00548	46	0.00172	85	0.00533
420	90	0.00553	54	0.00185	87	0.00500
480	91	0.00502	60	0.00191	93	0.00543

Table S5. Comparison of percentage degradation efficiency of MB dye by the ZnO nanostructures with literature values.

Material with Morphology	% Degradation efficiency	Time	Reference
ZnO Nanoparticles	81	180 min	70
ZnO Nanoparticles	92	180 min	70
Protein-capped ZnO nanoparticles	90	30 min	71
Ag/ ZnO Microrods	100	60 min	72
2% Fe-ZnO nanoparticles	92	180 min	73
Mn-ZnO nanoparticles	99	120 min	74
ZnO-bpma-12 (nanospheres)	91	480 min	<i>This work</i>
ZnO-bpea-12 (1D micro-rods)	60	480 min	<i>This work</i>
ZnO-bpta-12 (3D polyhedrons)	93	480 min	<i>This work</i>

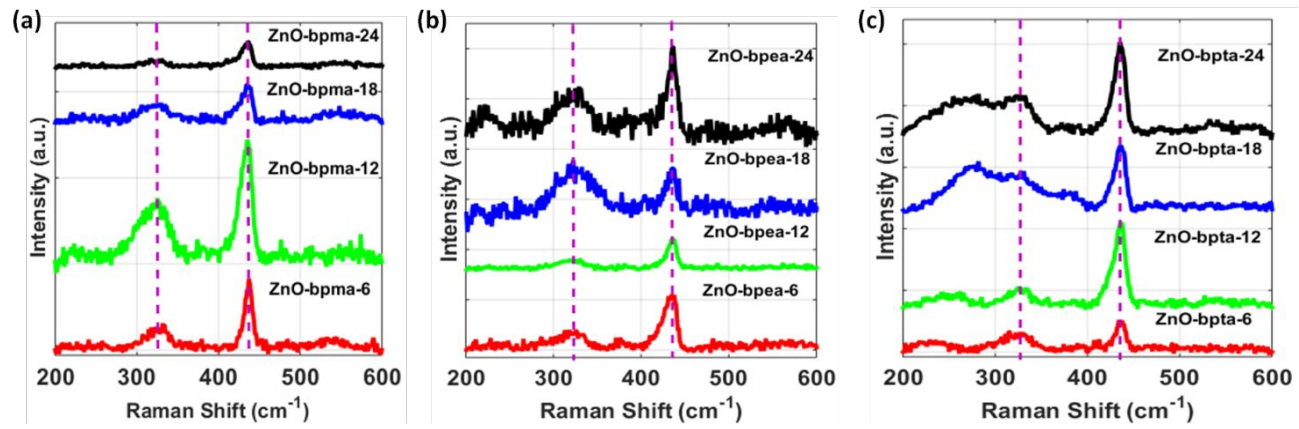


Figure S1. (a-c) Raman spectra of as-grown ZnO nanostructures.

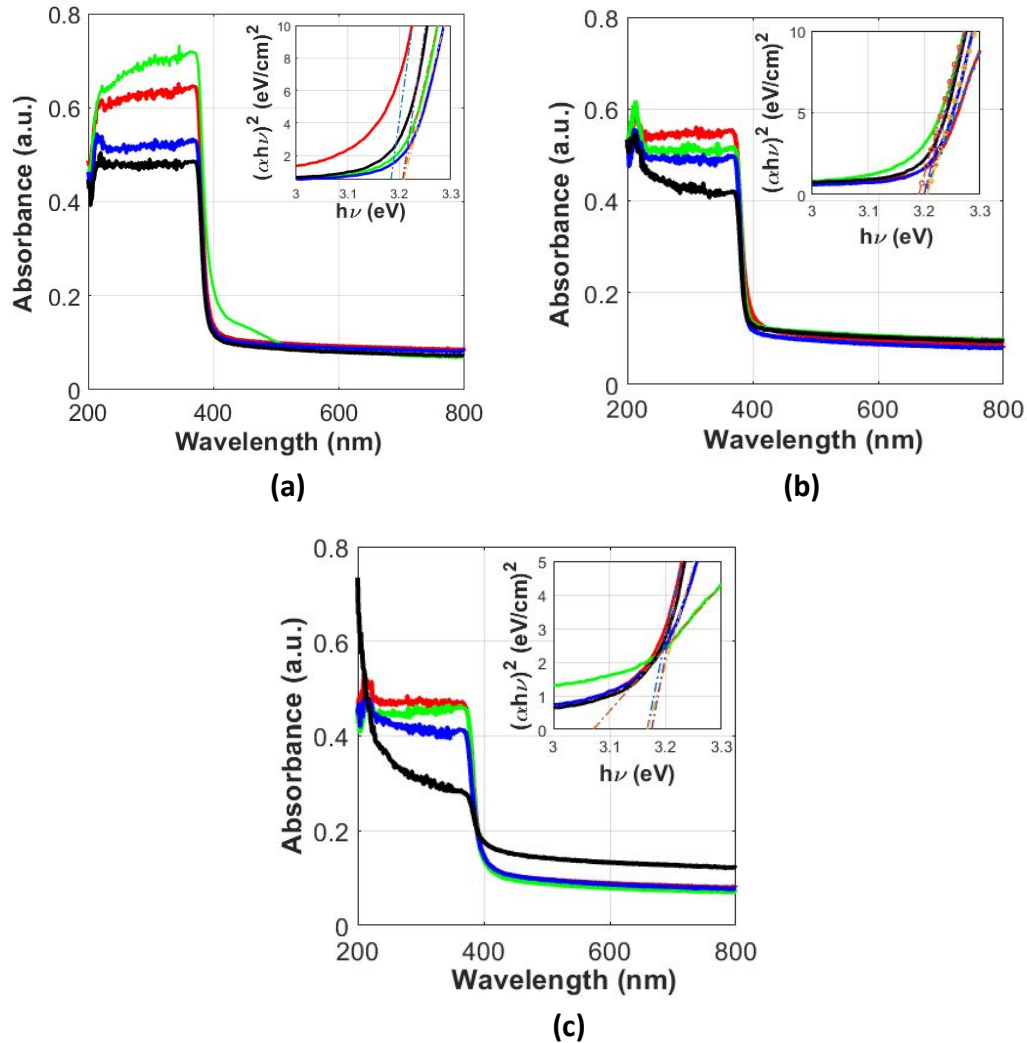


Figure S2. UV-vis diffuse reflectance spectra of (a) ZnO-bpma-t, (b) ZnO-bpea-t, (c) ZnO-bpta-t ($\{t = 6$ (red), $t = 12$ (green), $t = 18$ (blue) and $t = 24$ (black)), where inset is plot of $(\alpha h\nu)^2$ versus $(h\nu)$.

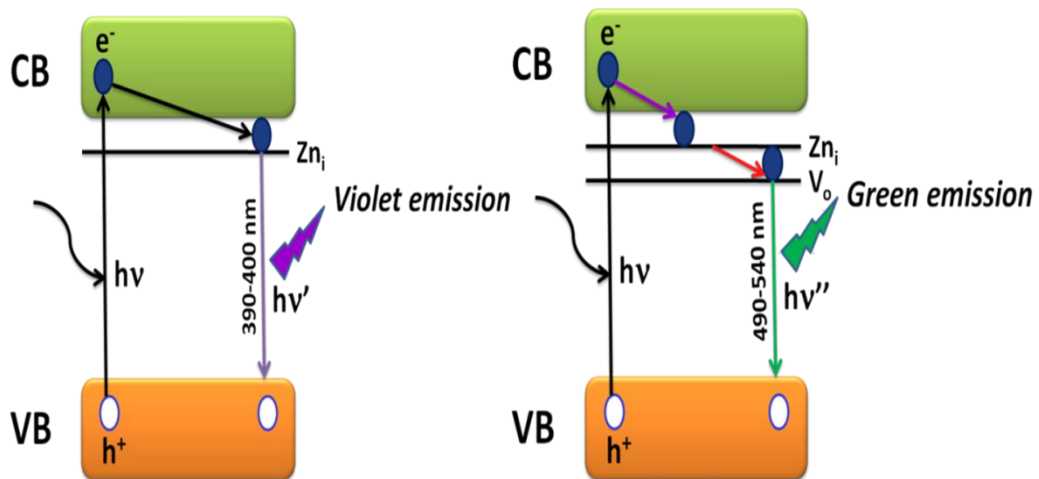


Figure S3. Energy level diagram for the as-synthesized ZnO.

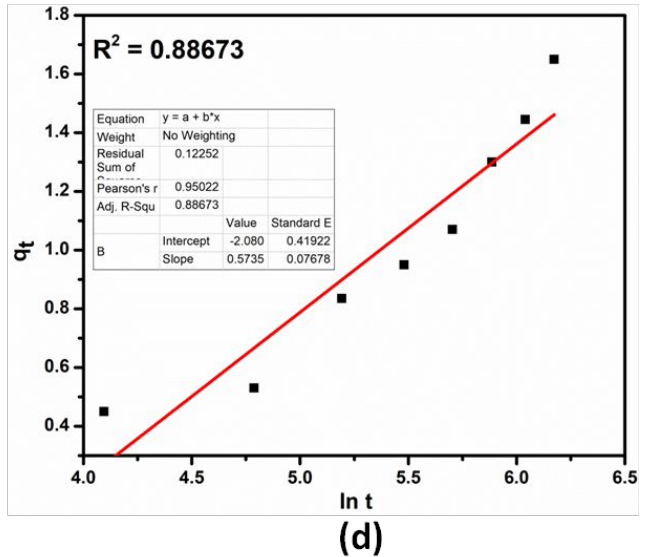
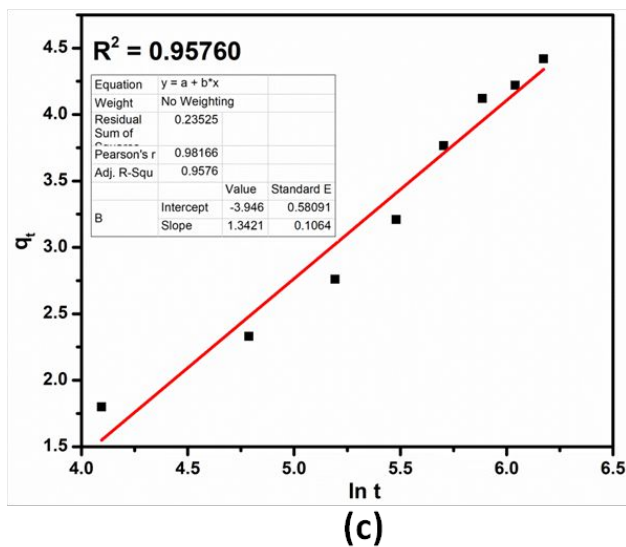
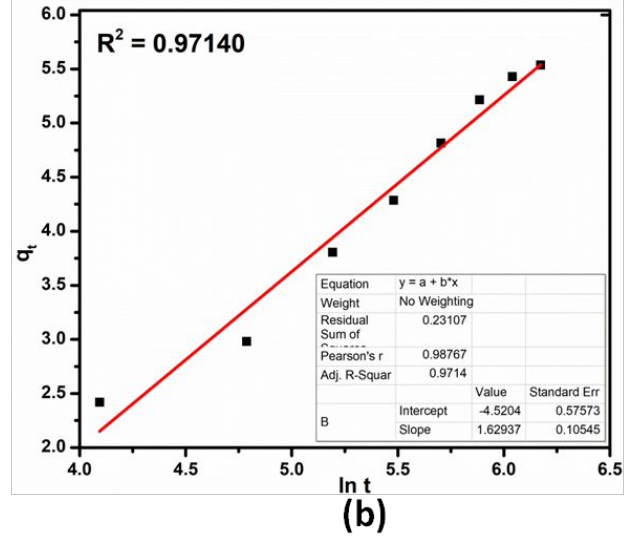
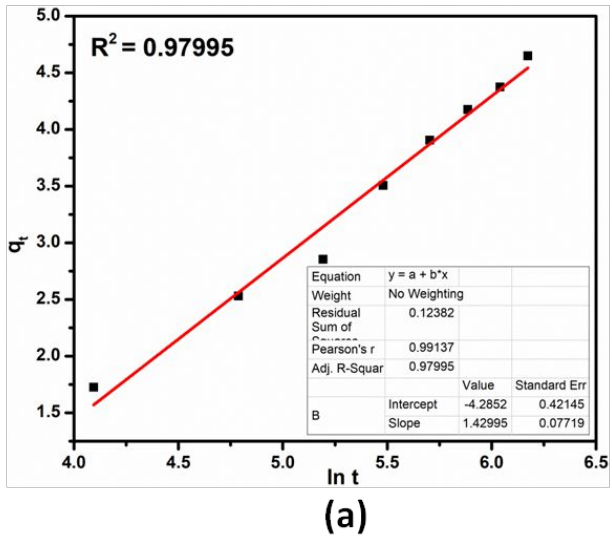


Figure S4. Elovich's kinetic model of (a) ZnO-bpma-6, (b) ZnO-bpma-12, (c) ZnO-bpma-18 and (d) ZnO-bpma-24 for the removal of MB dye.

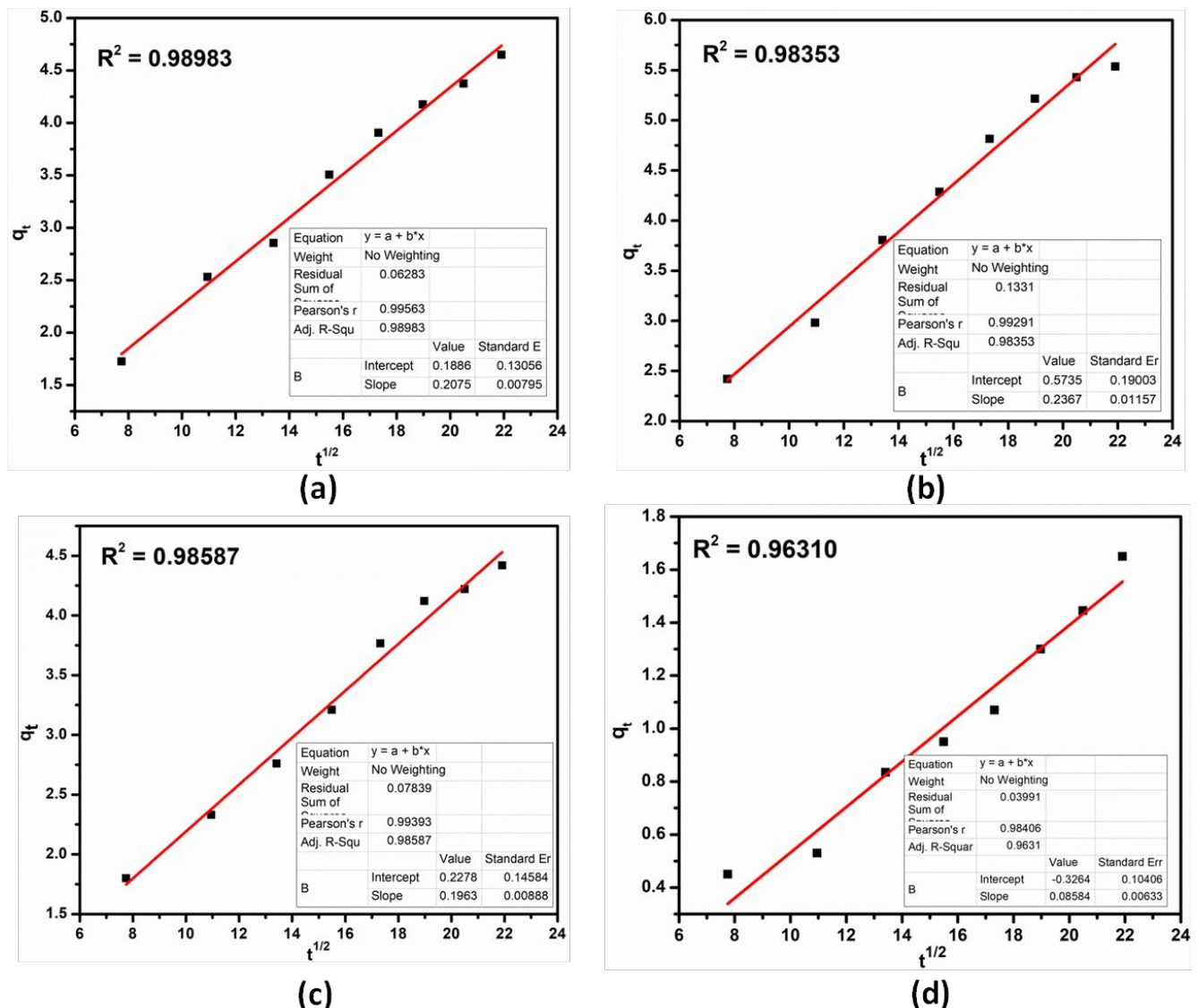


Figure S5. Intraparticle diffusion kinetic model of (a) ZnO-bpma-6, (b) ZnO-bpma-12, (c) ZnO-bpma-18 and (d) ZnO-bpma-24 for the removal of MB dye.

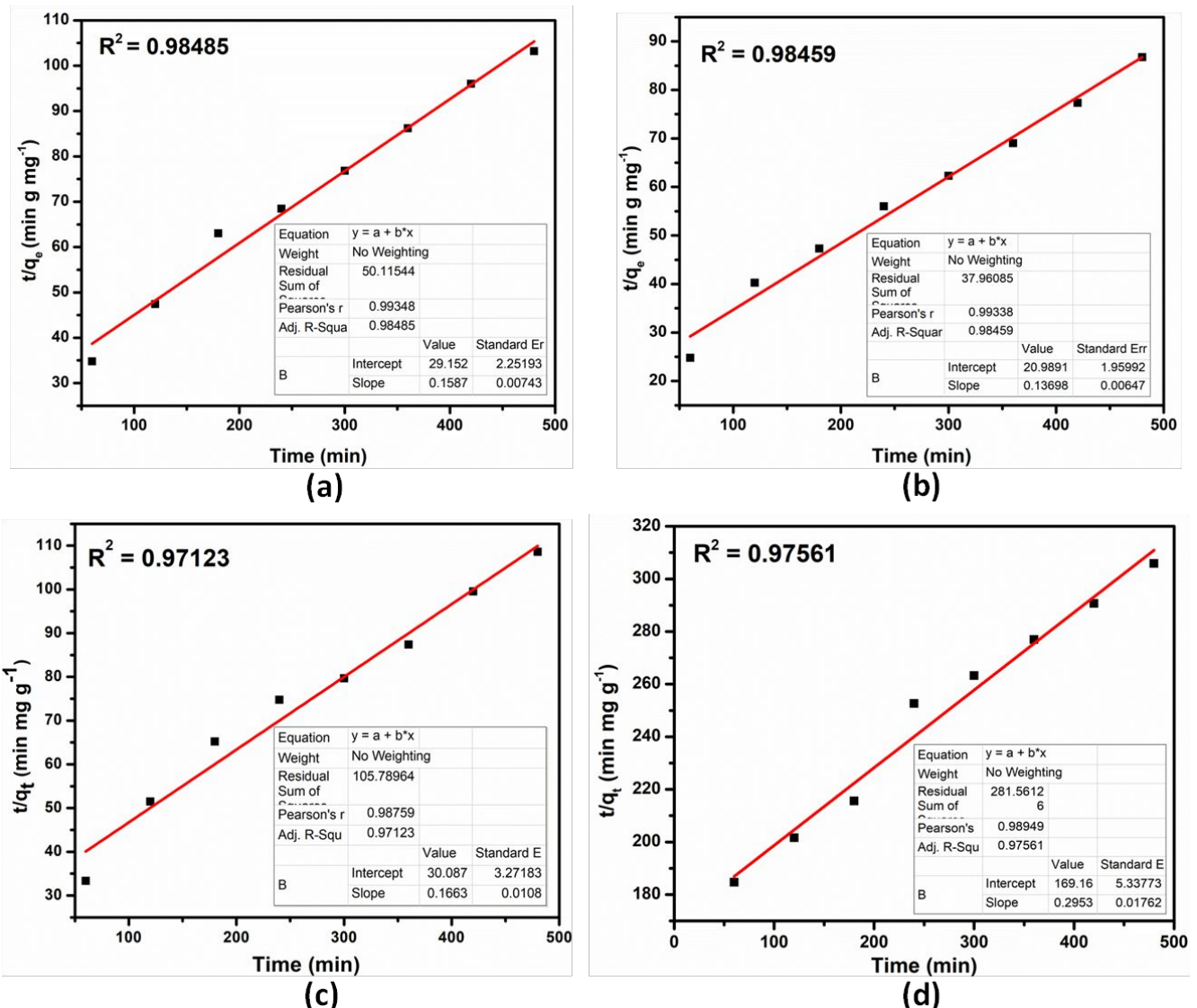


Figure S6. Pseudo-second-order kinetic model of (a) ZnO-bpma-6, (b) ZnO-bpma-12, (c) ZnO-bpma-18 and (d) ZnO-bpma-24 for the removal of MB dye.

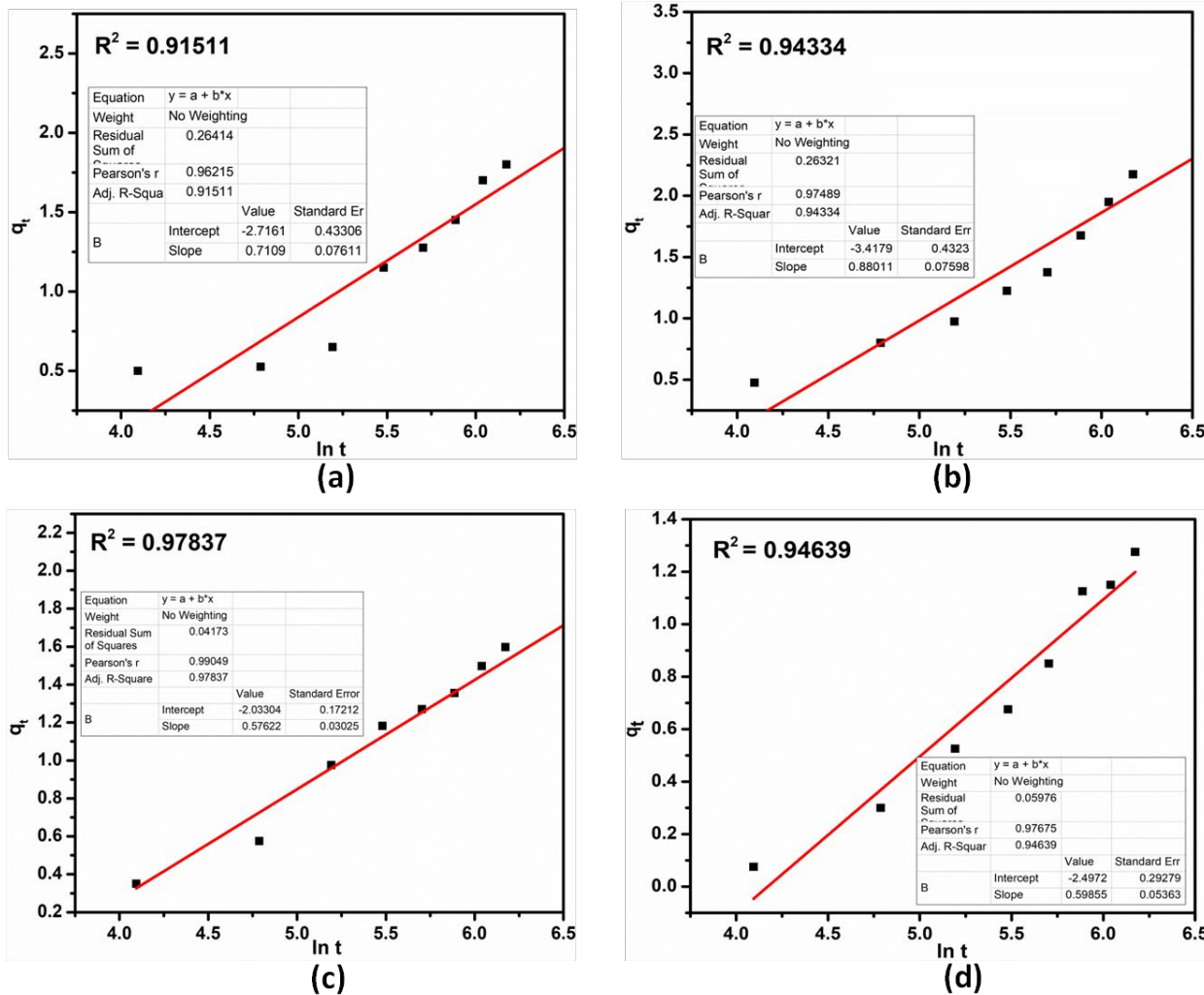


Figure S7. Elovich's kinetic model of (a) ZnO-bpea-6, (b) ZnO-bpea-12, (c) ZnO-bpea-18 and (d) ZnO-bpea-24 for the removal of MB dye.

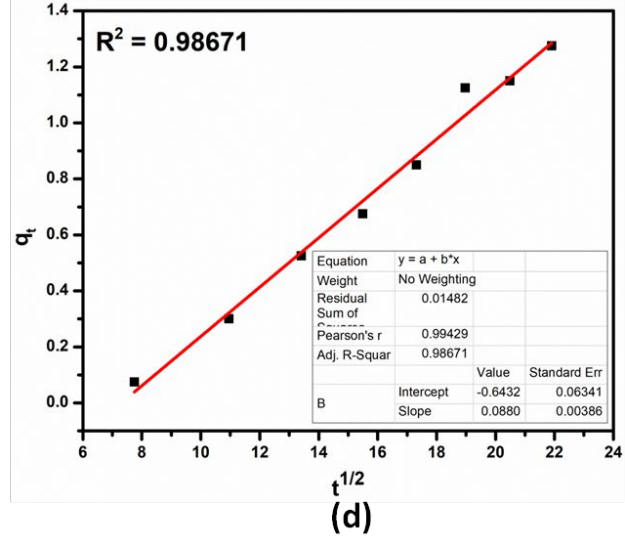
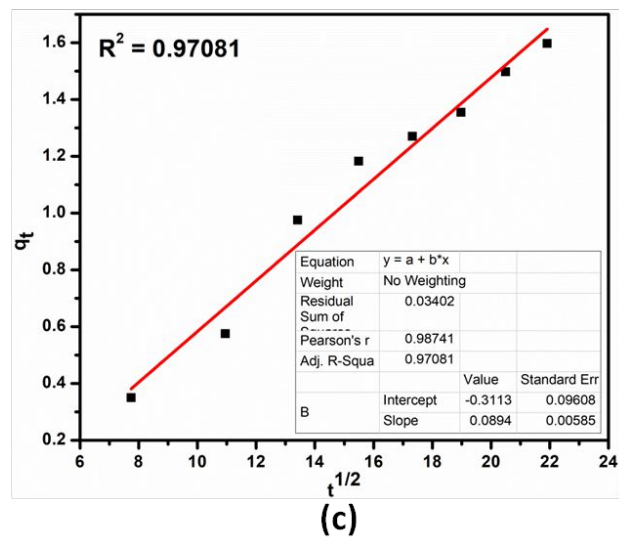
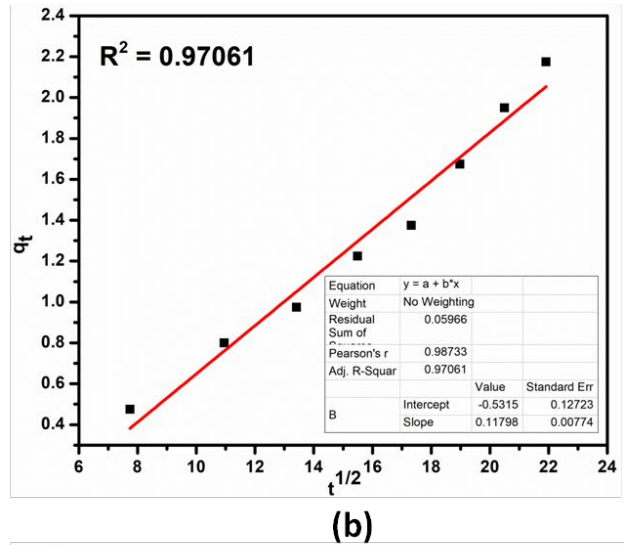
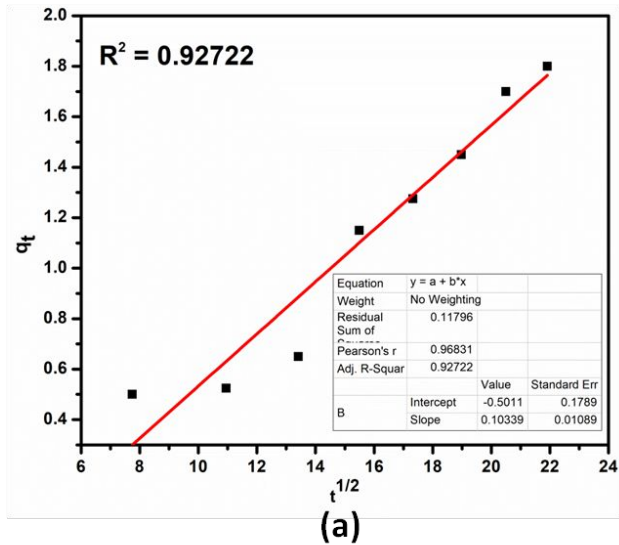


Figure S8. Intraparticle diffusion kinetic model of (a) ZnO-bpea-6, (b) ZnO-bpea-12, (c) ZnO-bpea-18 and (d) ZnO-bpea-24 for the removal of MB dye.

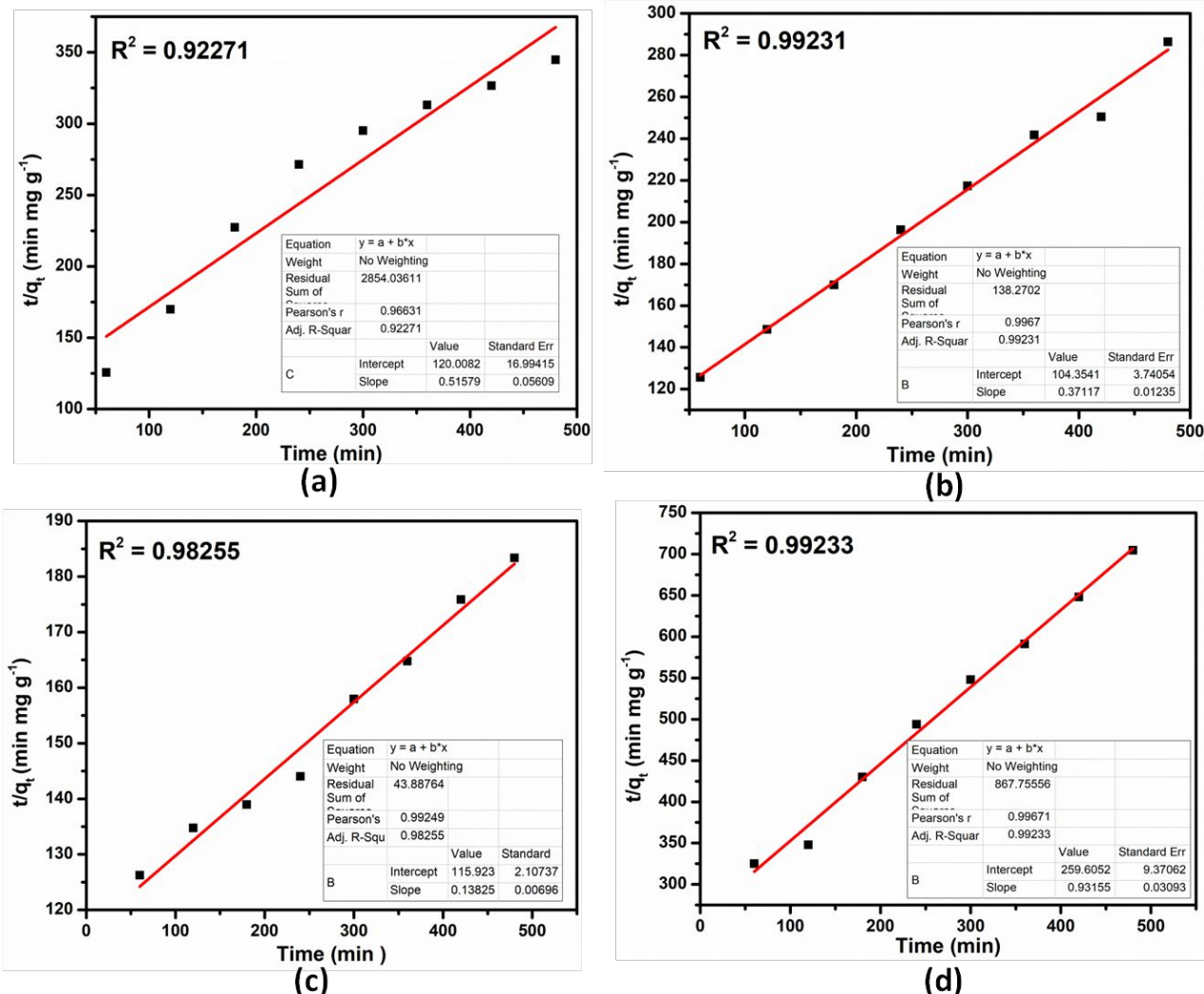


Figure S9. Pseudo-second-order kinetic model of (a) ZnO-bpea-6, (b) ZnO-bpea-12, (c) ZnO-bpea-18 and (d) ZnO-bpea-24 for the removal of MB dye.

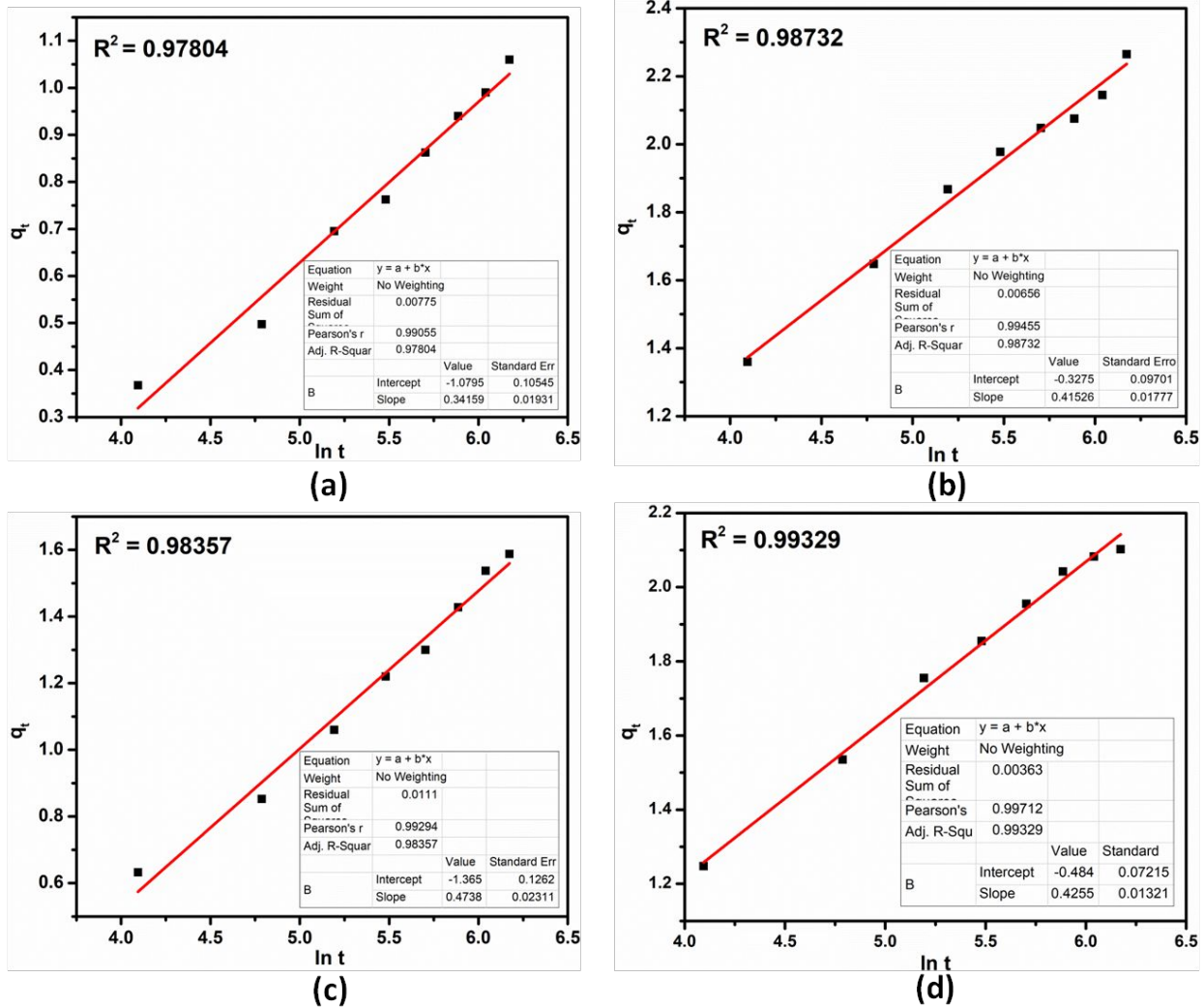


Figure S10. Elovich's kinetic model of (a) ZnO-bpta-6, (b) ZnO-bpta-12, (c) ZnO-bpta-18 and (d) ZnO-bpta-24 for the removal of MB dye.

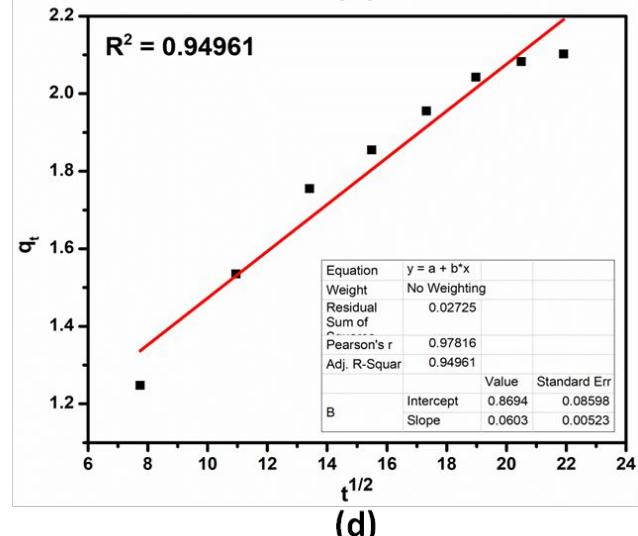
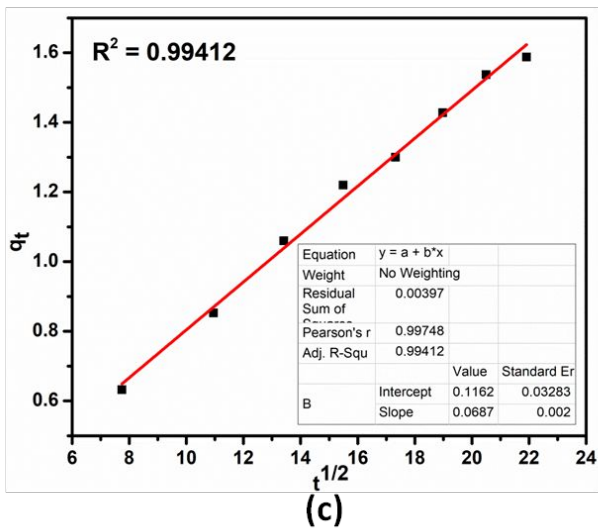
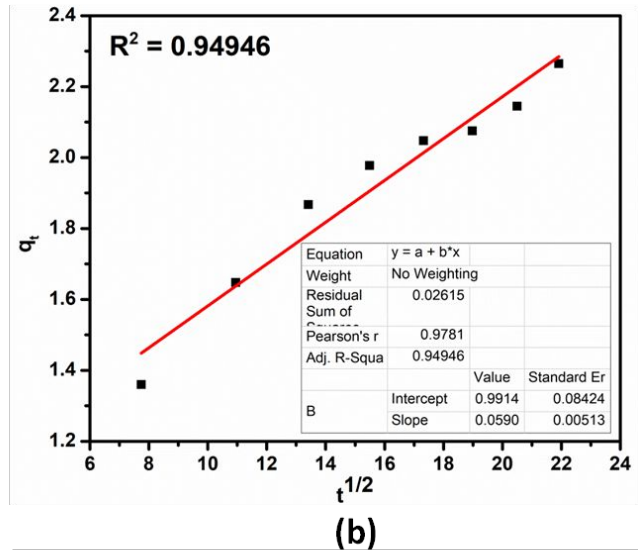
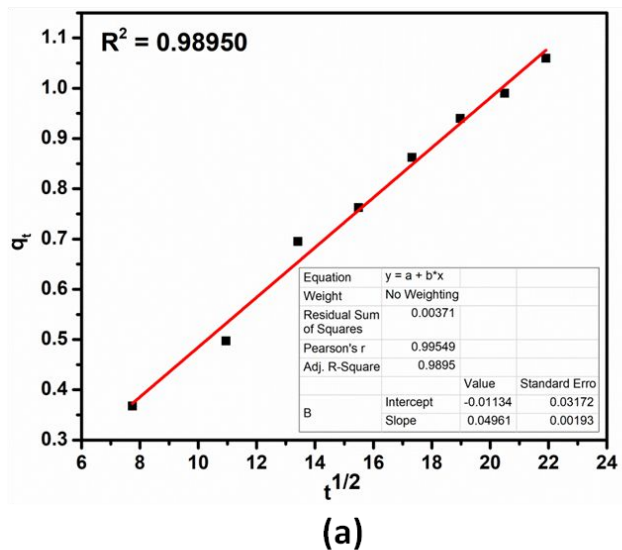


Figure S11. Intraparticle diffusion kinetic model of (a) ZnO-bpta-6, (b) ZnO-bpta-12, (c) ZnO-bpta-18 and (d) ZnO-bpta-24 for the removal of MB dye.

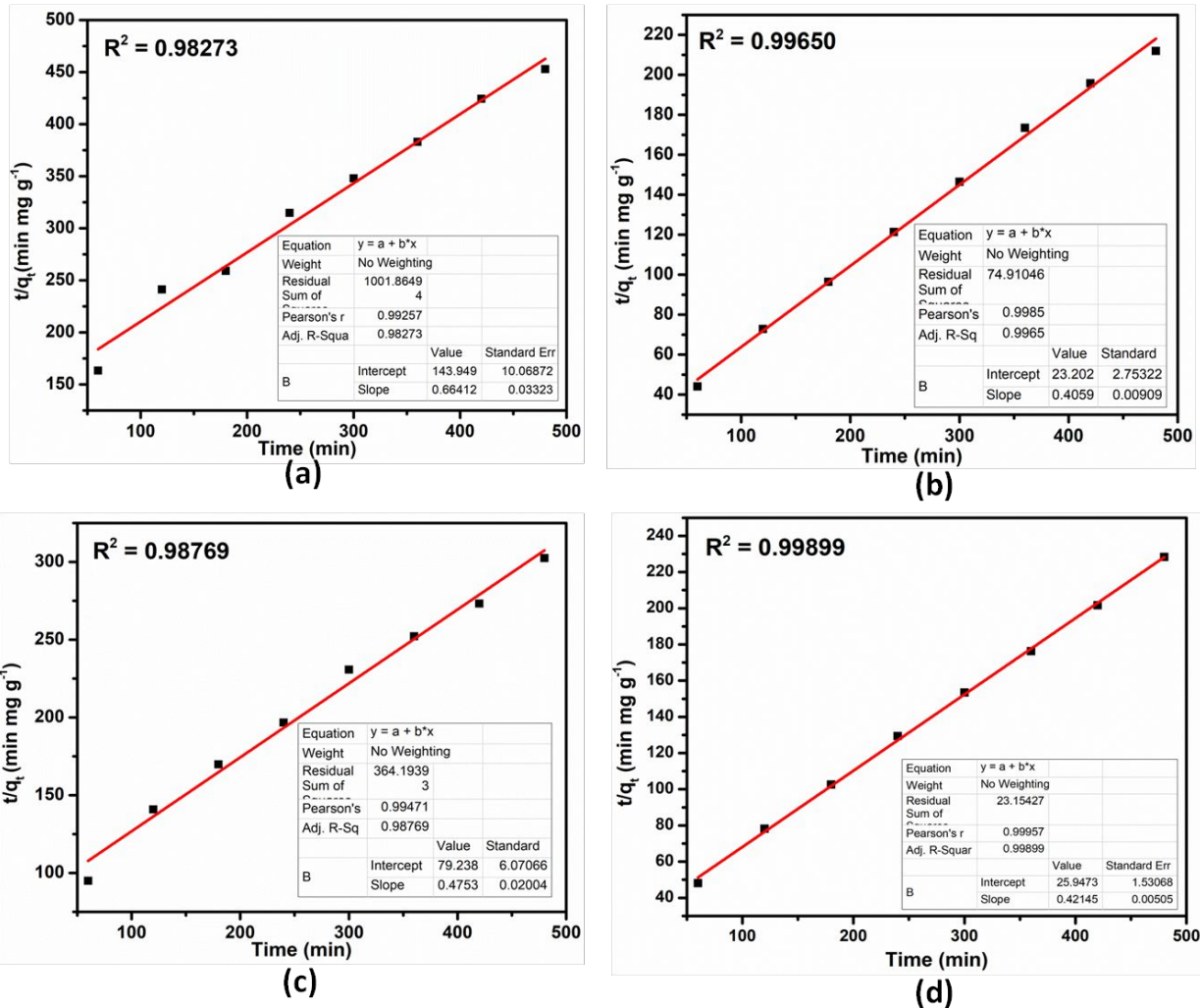


Figure S12. Pseudo-second-order kinetic model of (a) ZnO-bpta-6, (b) ZnO-bpta-12, (c) ZnO-bpta-18 and (d) ZnO-bpta-24 for the removal of MB dye.